Available online at www.sciencedirect.com
SCIENCE DIRECT®
Journal of Sound and Vibration 276 (2004) 919–932
JOURNAL OF SOUND AND VIBRATION
www.elsevier.com/locate/jsvi

Vibration suppression of plate using linear MR fluid passive damper

Tjahjo Pranoto, Kosuke Nagaya*, Atsushi Hosoda

Department of Mechanical Engineering, Gunma University, Kiryu, Gunma 376-8515, Japan

Received 1 August 2002; accepted 6 August 2003

Abstract

In order to suppress vibrations of large flexible structures such as aircraft wings, a damper will be applicable. Since eigenfrequencies of an aircraft wing are small, it requires the following for the damper: (1) The damping force have to be large for low frequency because the vibration frequency of the wing is small. (2) it works for small displacement, (3) its size has to be small which can be stacked in the wing, and (4) passive damper is desirable because the maintenance has to be free in the damper. This article presents a new type linear damper, which satisfies the conditions as just mentioned. The damper consists of a number of thin plates with slits. MR fluid is filled in the damper, so that magnetic fields freeze MR fluid. Resisting torque (shearing torque) is generated when the plates slide due to the shear of slits of the plates. The damper works against the bending moment of the wing by responding its deflection. The damper is maintenance free, and it is one of passive dampers with a good durability.

1. Introduction

In order to suppress vibrations of structures, various dampers have been presented [1–4]. Vibration absorbers using the dampers are used for suppressing vibrations, and a number of papers have been published [5–12].

An aircraft wing is usually made of aluminum alloy for making light aircraft. The aluminum alloy is light and strong, but its fatigue strength decreases with the number of vibrations. Finally, its strength becomes almost zero after a large number of vibrations. Hence, there is a life in the aircraft. When the stress amplitude is small, the life becomes long of course. Hence, it is of importance to decrease amplitude of vibration of the wing. In the aircraft, there are some restrictions, because the weight should be small, and wing should be strong. Hence, it is difficult to

*Corresponding author. Tel.: +81-277-30-1563; fax: +81-277-30-1567.
E-mail address: nagaya@me.gunma-u.ac.jp (K. Nagaya).

0022-460X/$ - see front matter © 2003 Elsevier Ltd. All rights reserved.
doi:10.1016/j.jsv.2003.08.019

use vibration absorbers in the wing, and so vibration control device has not been used in wings. However, when compact dampers are stacked in the wing without affecting wing strength, vibrations will be suppressed.

As for the damper, strain-type damper attached to the wing directly is desirable. The piezoelectric actuators are used for controlling vibrations of plates [12–16]. In those studies, piezoelectric ceramics are sandwiched between plates, so that, thickness of the plate is thin. However, It requires a complex control unit, and consumes control energy. In addition, maintenance is required. Recently, an electrorheological fluid damper has been developed, and effects of the fluid on the damping force have been investigated [17–19]. The damper has strong damping force, and so it has been used for attenuating vibrations of machines and structure. Choi et al. [20–22], and Wang et al. [23] discussed vibration control of structures. In the studies, it was ascertained that vibration suppression was enough when using ER damper. However, although the damper is useful for controlling vibrations for structures, it also consumes electric energy.

A passive damper without consuming electric energy is desirable for an aircraft wing because it requires no maintenance. The strain-type damper is also required when it is used as the aircraft damper. The ordinary piston-type damper does not work for small displacement due to an air in the damper. In addition, the damping force of the damper is in proportion to velocity. First eigenfrequency of aircraft wing is low, so that the damping force in the first mode is significantly small for the damper. Then, it is inadequate as the aircraft damper. Recently, a MR fluid damper has been presented [24–26]. It is also the piston-type damper, and so it has the same disadvantages as just mentioned. From this situation, a new strain-type shear damper is provided in this paper, which does not consume control energy. Hence, the damper is the passive type. The damper consists of permanent magnets and a number of plates with slits. Driving plates and follower plates are sandwiched by turns, and hence large shearing force can be obtained at the slits when a sliding motion occurs between driving plates and follower plates. The damper is made, and its resisting force is measured. Effects of the damper on vibration suppression of the plates are investigated experimentally. The analytical discussion is also made.

2. Development of MR fluid linear damper

2.1. Construction of MR fluid linear damper

Since the aircraft wing is long, its eigenfrequency is significantly small. In order to control such wings, a moment-type damper is desirable which can be pasted to the inside surface of the wing. Hence, in the damper for controlling vibration of aircraft wings, the following requirements have to be satisfied.

(1) The damper is thin and light which can be stacked without damaging the honeycomb structure of the wing.
(2) The damper has large resisting force for low frequency vibrations.
(3) The damper works for small displacement.

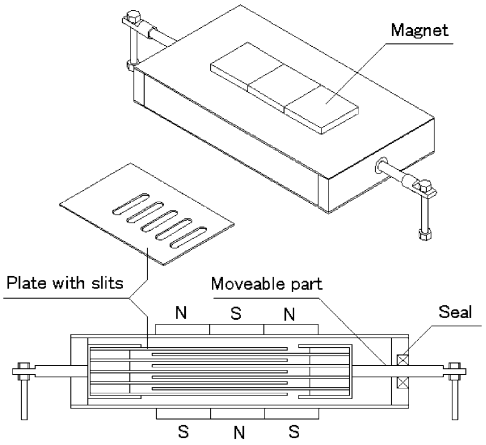

Fig. 1. Geometry of the MR-fluid damper.

(4) The damper can be used under maintenance free, and has good durability (a passive damper is desirable).
(5) The damper, which does not consume control energy, is desirable.

An ordinary hydraulic damper using orifice effect cannot satisfy condition (3) because air in it is compressed, in addition, condition (2) cannot be satisfied, because the damping is small for low frequency vibrations. The rubber damper also does not work in small frequency region. The magnetic damper works for small displacement. In the damper, however, condition (2) cannot be satisfied, because its damping force is also small for low frequency vibrations. The electrorheological fluid-filled laminate composite [20–22] satisfies (1)–(4), but (5) cannot be satisfied, because it consumes electric energy. Hence, the new type damper is desirable for controlling aircraft wings.

In this article, we propose the damper which covers above-mentioned all conditions. The damper (Fig. 1) contains plates with slits, one group fixed and the other moveable, alternately installed in a thin rectangular box. The box is made of acrylic and aluminum plate, filled with MR fluid which is protected from leakage by seal. Permanent magnets are put on above and under sides of the box with opposites pole configuration, so that the presence of magnetic induction freezes the MR fluid and magnetic pillars through the slits are formed. The damper is set on the plate surface. Movement of the plate will squeeze (cut) the magnetic pillar in the damper, and shear force can be gained. The resisting force due to shear motion is almost constant, and has no dependence on the frequency. This is the essential difference from the piston-type dampers.

2.2. Analysis of resisting forces

There occur resisting forces in the damper due to friction force of seal, friction force between plate surfaces and MR fluid, shear force gained from slits, and viscose damping. The resisting force due to the magnetic fields can be assumed as quadratic of the magnetic flux density, thus:

$$f_m(x) = B(x)^2 g_0, \tag{1}$$

where g_0 is the friction force per unit area under unit magnetic flux density. Thus, the friction force F_m is

$$F_m = 2Nb \int_0^a f_m(x)\,\mathrm{d}x, \tag{2}$$

where $B(x)$ is the magnetic flux density, N the number of moveable plate, a the length of the plate, b the width of the plate.

As mentioned above, permanent magnets are put on both sides (above and under) so that magnetic flux flows through the (inner) part of the damper (slits) with pole configuration $\mathrm{N,S,N}\cdot\cdot\cdot$. If this configuration reverses, a gradient of magnetic flux becomes higher, and this causes higher shearing force at the slits. For numerical calculation, this shear force may be assumed as a constant shear force as follows:

$$F_s = NC_0 \sum_{s=1}^{n} f_s, \tag{3}$$

where

$$f_s = B(x_s)^2 g_1. \tag{4}$$

C_0 is the effective shear length per slit, n is the slit number for a plate, and g_1 is the shear force per unit magnetic flux density, and subscript s denotes the sth slit. The friction area decreases when there are slits. The effect is

$$F_s' = 2C_1C_2N \sum_{s=1}^{n} f_m(x_s), \tag{5}$$

where C_1 is the slit width, and C_2 the slit length. Let F_0 be the friction force due to seals, the total resisting force becomes:

$$\begin{aligned} F &= F_0 + F_m + F_s - F_s' \\ &= F_0 + 2Nb \int_0^a f_m(x)\,\mathrm{d}x + NC_0 \sum_{s=1}^{n} f_s(x_s) - 2C_1C_2N \sum_{s=1}^{n} f_m(x_s). \end{aligned} \tag{6}$$

There is also the resisting force due to viscosity of MR fluid. The force can be written by

$$F_c = C\,\mathrm{d}x/\mathrm{d}t, \tag{7}$$

where C is the damping coefficient, x the displacement, and t the time.

2.3. Numerical calculation and experimental check for the resisting force

An MR damper was made as shown in Fig. 1. The resisting force for this type of dampers can be calculated by the method as mentioned below. In the calculation of the resisting force, the following four coefficients should be decided first: The friction force F under non-magnetic field, friction stress g_0 when the magnet lies, shear force g_0 due to a slit, and damping coefficient C.

2.3.1. Decision of F_0 and g_0

The MR fluid is filled in the damper box whose viscosity is 1.99 Pa s (see Fig. 1). The friction force F_0 without MR fluid was obtained as $F_0 = 1.75$ (N) experimentally. The friction stress of the

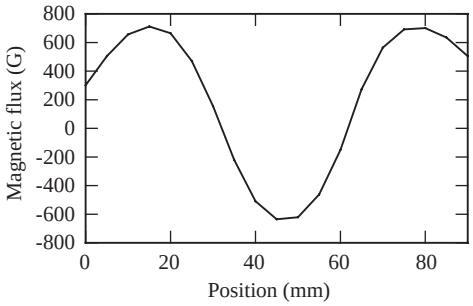

Fig. 2. Magnetic flux distribution.

MR fluid is obtained using three sandwiched rectangular plates, but the MR fluid is filled in the gaps among the plates. The friction force is obtained as $F_m = 0.06$ (N).

The magnetic flux density $B(x)$ is shown in Fig. 2 when N and S poles of the magnets are arranged by turns. It can be written as

$$B(x) = 712 \sin(4x + 25). \tag{8}$$

Substituting Eq. (8) into Eqs. (1) and (2), yield

$$g_0 = F_m \Big/ \left\{ 2Nb \int_0^a 712^2 \sin^2(4x + 25)\, \mathrm{d}x \right\}, \tag{9}$$

where the unit of angle is degree. Using Eq. (9), we have $g_0 = 2.2 \times 10^{-11}$ (N/mm^2 G).

2.3.2. Decision of g_1

In order to have g_1, three sandwiched rectangular plates with slits are used. The MR fluid is also filled in the gaps of the plates. The shearing force at the slit is obtained by the equation $F_s (= W - F_0 - F_m + F_s')$, where W is the total resisting force under the magnetic field. W is measured as $W = 6.5$ (N), and using Eqs. (1) and (5) and Fig. 2, we get $F_s' = 11 \times 10^{-3}$ (N) . Then we have $F_s = 4.8$ (N). The coefficient g_0 is calculated from Eqs. (3) and (4) and Fig. 2:

$$g_1 = F_s \Big/ \left\{ NC_0 \sum_{s=1}^{n} B(x_s)^2 \right\}. \tag{10}$$

Eq. (10) gives $g_1 = 9.54 \times 10^{-8}$ (N/mm G).

2.3.3. Damping force

In order to have the damping coefficient due to MR fluid (without magnet), the damper is mounted to a thin beam. The damping coefficient due to viscosity of MR fluid was obtained by a usual free vibration method. Obtained damping ratio is

$$\zeta = c/(2\sqrt{kM}) = 0.015,$$

where k is the spring constant of the beam at the position of the damper and M is the mass of the damper. The damping coefficient due to viscosity without magnet is small in comparison with the shear force.

2.3.4. Resisting force for the MR damper

The MR fluid damper made in this research has 155 mm in length, 85 mm in width, and 30 mm in thickness. Rectangular plates are stacked, whose length $a = 90$ mm, width $b = 60$ mm and thickness $h_d = 1$ mm. The fixed plates and sliding plates (movable plates) are sandwiched by turns. The number is 5 for fixed plates, and 4 for sliding plates. The width of the slit is $C_1 = 6$ mm, and length of the slit is $C_2 = 30$ mm, effective shear length of the slit involving the rounds is $C_0 = 36$ mm, and the number of slit for a plate is $n = 5$ (see Fig. 1).

Using above equations, the resisting force F can be calculated by Eq. (6). The calculated force is $F = 6.6$ N for the MR damper with a pair of magnets, while the experimental result is $F = 6.5$ N. The result for 3 pairs of magnets is also calculated. The theoretical force is $F = 21.9$ N, and experimental force is $F = 21.79$ N. Theoretical results are in good agreement with the experimental. Then, the resisting force involving the shearing force for the present damper is calculated by using the fundamental experiment as just mentioned.

3. Plate vibration suppression using the MR damper

As an application of the MR damper, consider plate vibration control problem as shown in Fig. 3. The damper is fixed on the plate and making angle θ to the x-axis. Point ($x = x_j$, $y = y_j$) displaces with transverse vibration movement $w(t)$ due to load $Q_s(t)$. Using co-ordinate as describes in Fig. 3, equation of motion becomes:

$$\begin{aligned} D\nabla^2 w + \rho h\frac{\partial^2 w}{\partial t^2} + \sum_{i=1}^{2}\frac{M}{2}\frac{\partial^2 w}{\partial t^2}\,\delta(x-\bar{\eta}_i)\delta(y-\bar{\delta}_i) \\ = m_x\{\delta'(x-\bar{\eta}_2)\delta(y-\bar{\delta}_2) - \delta'(x-\bar{\eta}_1)\delta(y-\bar{\delta}_i)\} \\ + m_y\{\delta(x-\bar{\eta}_2)\delta'(y-\bar{\delta}_2) - \delta(x-\bar{\eta}_1)\delta'(y-\bar{\delta}_1)\} \\ + \sum_{s=1}^{s} Q_s(t)\delta(x-x_s)\delta(y-y_s), \end{aligned} \tag{11}$$

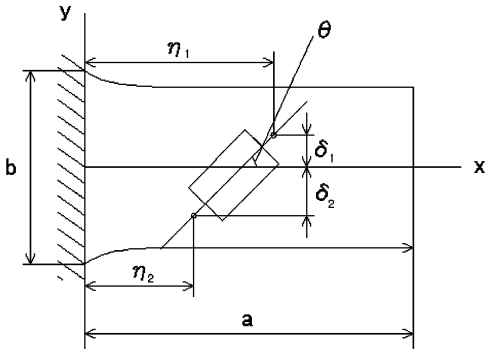

Fig. 3. Cantilever plate with MR-fluid damper.

where

$$\nabla^4 = \frac{\partial^4 w}{\partial x^2} + 2\frac{\partial^4 w}{\partial x^2 \partial y^2} + \frac{\partial^4 w}{\partial y^4},$$

$$D = \frac{Eh^3}{12(1-v^2)}$$

and where, E is Young's modulus of the plate, ρ the mass density of the plate, v the Poisson ratio, $h$the thickness, M the mass of the damper, w the displacement of the plate, D the bending stiffness, t the time, m_x the moment around x-axis generated by the present damper, and m_y the moment around y-axis. $\delta(x-\bar{\eta}i)$ and $\delta(y-\bar{\delta}i)$ are Dirac's delta functions which represent the forces generated by the damper, and $\delta'(x-\bar{\eta}i)$ and $\delta'(y-\bar{\delta}i)$ are the doublet functions which represent the moments generated by the damper.

Consider the displacement functions $\phi_m(X)$ and $\psi_n(Y)$ $(X = x/a,\ Y = y/l)$. The displacement of the plate is expanded in the following form:

$$w = \sum_{m=1}^{\infty}\sum_{n=1}^{\infty} f_{mn}\phi_m(X)\psi_n(Y)\,\mathrm{e}^{\mathrm{i}\omega t}, \tag{12}$$

where ω is the exciting circular frequency, f_{mn} is the coefficient, and $\mathrm{i} = \sqrt{-1}$. The geometrical boundary conditions of the plate may be assumed as combination of a clamped–free (in x direction) and free–free (in y direction) beam. The displacement functions used in this paper are presented in the appendix.

The vibration force can be written as

$$P_s = Q_s\,\mathrm{e}^{\mathrm{i}\omega t}, \tag{13}$$

where Q_s is the amplitude of the sth external force. Bending slope of the plate at the damper position at $X = \eta_j,\ Y = \delta_j$ $(\eta_j = \bar{\eta}_j/a,\ \ \delta_j = \bar{\delta}_j/l)$ is

$$\left(\frac{\partial w}{\partial x}\right)_{X=\eta_j, Y=\delta_j} = \sum_{m=1}^{\infty}\sum_{n=0}^{\infty}\left(\frac{1}{a}\right) f_{mn}\phi_m(\eta_j)\psi_n(\delta_j)\,\mathrm{e}^{\mathrm{i}\omega t}. \tag{14}$$

Consider the height of actuator leg H from the mid-plane of the plate to the actuator rod of the damper (see Fig. 1), the relative displacement between both legs of the damper can be found and its relative velocity is

$$v = \sum_{m=1}^{\infty}\sum_{n=0}^{\infty}\left(\frac{H}{a}\right)\mathrm{i}\omega f_{mn}\left\{\phi_m^{(1)}(\eta_2)\psi_n(\delta_2) - \phi_m^{(1)}(\eta_1)\psi_n(\delta_1)\right\}\mathrm{e}^{\mathrm{i}\omega t}. \tag{15}$$

In the following, considering only the amplitude ($\mathrm{e}^{\mathrm{i}\omega t}$ is neglected), the damper force u_x in x direction becomes:

$$u_x = -F_x - C_x\sum_{m=1}^{\infty}\sum_{n=0}^{\infty}\left(\frac{H}{a}\right)\mathrm{i}\omega f_{mn}\left\{\phi_m^{(1)}(\eta_2)\psi_n(\delta_2) - \phi_m^{(1)}(\eta_1)\psi_n(\delta_1)\right\} \tag{16}$$

in y direction, u_y:

$$u_y = -F_y - C_y\sum_{m=1}^{\infty}\sum_{n=0}^{\infty}\left(\frac{H}{l}\right)\mathrm{i}\omega f_{mn}\left\{\phi_m(\eta_2)\psi_n^{(1)}(\delta_2) - \phi_m(\eta_1)\psi_n^{(1)}(\delta_1)\right\}. \tag{17}$$

The moments are $m_x = u_x H$ and $m_y = u_y H$. Substituting Eqs. (12), (13), (16) and (17) into Eq. (11), multiplying by $\phi_p(X)$, $\psi_q(Y)$ and integrating with consideration of the orthogonal condition in $\phi_m(X)$ (but not in $\phi_n(Y)$), one gets the following equation:

$$\sum_{n=0}^{\infty}(H_{mnq} - \gamma^4 Q_{mnq} + \mathrm{i}\omega G_{mnq}) f_{mn}^* = Q_0^* \left(\frac{a}{b}\right) \phi_m(X_0)\psi_q(Y_0)$$
$$(m = 1, 2, \ldots, \infty, \quad q = 1, 2, \ldots, \infty), \tag{18}$$

where

$$\begin{aligned}
H_{mnq} = {} & \int_{-1}^{1}\int_{0}^{1}\left\{\left(\frac{l}{b}\right)\phi_m^{(4)}(X)\phi_m(X)\psi_n(Y)\psi_q(Y)\right. \\
& + 2\left(\frac{b}{l}\right)\left(\frac{a}{b}\right)^2 \phi_m^{(2)}(X)\phi_m(X)\psi_n^{(2)}(Y)\psi_q(Y) \\
& \left. + \left(\frac{b}{l}\right)^3\left(\frac{a}{b}\right)^4 \phi_m^2(X)\psi_n^{(4)}(Y)\psi_q(Y)\right\} \mathrm{d}X\,\mathrm{d}Y, \\
Q_{mnq} = {} & \int_{-1}^{1}\int_{0}^{1}\left(\frac{l}{b}\right)\phi_m^2(X)\psi_p(Y)\psi_q(Y)\,\mathrm{d}X\,\mathrm{d}Y \\
& + \sum_{j=1}^{2}\frac{M_j^*}{2}\left\{\phi_m^2(\eta_j)\psi_n(\delta_j)\psi_q(\delta_j)\right\}, \\
G_{mnq} = {} & \left(\frac{a}{b}\right)A_{mn}\left\{\phi_m^{(1)}(\eta_2)\psi_q(\delta_2) - \phi_m^{(1)}(\eta_1)\psi_q(\delta_1)\right\} \\
& + \left(\frac{a}{b}\right)^2 B_{mn}\left\{\left(\frac{b}{l_2}\right)\phi_m(\eta_2)\psi_q^{(1)}(\delta_2) - \phi_m(\eta_1)\psi_q^{(1)}(\delta_1)\left(\frac{b}{l_1}\right)\right\}
\end{aligned} \tag{19}$$

and where

$$\begin{aligned}
& f_{mn}^* = \frac{f_{mn}}{a}, \quad Q_0^* = Q_0\frac{a}{D}, \quad M_j^* = \frac{M_j}{\rho h a b}, \quad X = \frac{x}{a}, \\
& Y = \frac{y}{l}, \quad \gamma^4 = \frac{\rho h \omega^2 a^4}{D}, \\
& A_{mn} = \left(\frac{Ha}{D}\right)(C_v + C_f)\left(\frac{H}{a}\right)\left\{\phi_m^{(1)}(\eta_2)\psi_n(\delta_2) - \phi_m^{(1)}(\eta_1)\psi_n(\delta_1)\right\}, \\
& B_{mn} = \left(\frac{Ha}{D}\right)(C_v + C_f)\left\{\left(\frac{H}{l_2}\right)\phi_m(\eta_2)\psi_n^{(1)}(\delta_2) - \left(\frac{H}{l_1}\right)\phi_m(\eta_1)\psi_n^{(1)}(\delta_1)\right\}.
\end{aligned} \tag{20}$$

Eq. (18) is written in matrix form

$$[a_m]\{f_m^*\} = \{P_m\}, \tag{21}$$

where

$$\begin{aligned}
& a_{mqn} = H_{mnq} + (\mathrm{i}\omega G_{mnq} - \gamma^4 Q_{mnq}), \\
& P_{mn} = Q_0^*\left(\frac{a}{b}\right)\phi_m(x_0)\psi_q(y_0).
\end{aligned} \tag{22}$$

From Eq. (21), we obtain $f^*_{m1} \sim f^*_{mn}$ and the displacement of the plate becomes:

$$w = a\sum_{m=1}^{\infty}\sum_{n=0}^{\infty}\phi_m(X)\psi_n(Y)f^*_{mn}\mathrm{e}^{\mathrm{i}\omega t}. \tag{23}$$

The damper presented here is one of the friction-type dampers, so that the resisting force is constant. In order to treat the force, we consider an equivalent damping. The equivalent damping coefficients C_f and C_v are written by $C_e = 4F/(\pi A\omega)$, where F is the friction force. If the damper is fixed with angle θ to the x-axis, vector of this friction force becomes:

$$\left.\begin{aligned} F_x &= F\cos\theta, \\ F_y &= F\sin\theta, \end{aligned}\right\} \tag{24}$$

Hence, the equivalent damping coefficients of the viscosity in x and y direction, become:

$$C_{\mathrm{e}x} = \frac{4F_x}{\pi A_x\omega}, \quad C_{\mathrm{e}y} = \frac{4F_y}{\pi A_y\omega}. \tag{25}$$

Here, A_x and A_y are vibration amplitudes of the damper obtained from Eq. (14);

$$\left.\begin{aligned} A_x &= \textstyle\sum_{m=1}^{\infty}\sum_{n=0}^{\infty} Hf^*_{mn}\{\phi^{(1)}_m(\eta_2)\psi_n(\delta_2) - \phi^{(1)}_m(\eta_1)\psi_n(\delta_1)\}, \\ A_y &= \textstyle\sum_{m=1}^{\infty}\sum_{n=0}^{\infty} Hf^*_{mn}\{\phi_m(\eta_2)\psi^{(1)}_n(\delta_2) - \phi_m(\eta_1)\psi^{(1)}_n(\delta_1)\}. \end{aligned}\right\} \tag{26}$$

Since Eq. (25) has amplitudes of the damper, the equivalent damping coefficients cannot be decided directly. Then, A_x and A_y are first assumed, and repeating the calculation of Eq. (23) through Eq. (26), ΔA is found in the equation $A_{xn} = A_{x,n-1} + \Delta A$, where A_{xn} is the value A_n in the nth calculation. The same calculation is also performed for A_{yn} until the value w being converged.

4. Experimental and numerical results

4.1. Experimental set-up

A rectangular aluminum plate is used in the experiment, whose length is 0.675 m, width is 0.3 m, and thickness is 2 mm. The MR damper with the mass 1.75 kg, height of leg $H = 20$ mm is mounted to the plate. Two types of mounting are chosen. (a) One is used for suppressing bending vibration, whose mounting points (co-ordinates) of two legs of the damper are (20, 0) mm, and (240, 0) mm. The exciting point is (665, 0) mm, and measuring point is (515, 0) mm. (b) The other is used for suppressing bending–torsion vibrations. The mounting points of the legs are (200, −80) mm, (340, 80) mm (see Fig. 3) in which the axis of the damper has the angle 45° with respect to the central axis of the plate, because the 45° line on the surface has maximum deformation in torsional deflection. The exciting point is (665, 150) mm, and the measuring point is (515, 150) mm.

A vibration pick up is put on the point at the measuring point as just mentioned. The impulse hammer hits the exciting point, and vibration pick up detects vibration signals of the plate. The signal is analyzed by the FFT, then, the displacement in the plate under a unit exciting force (1 N) is calculated.

In order to predict the performance of the damper, numerical result is compared with experimental one. Numerical calculations are carried out for the same plate used in the experiment whose Young's modulus is assumed to be $E = 7.2 \times 10^{10}$ Pa, mass density

$\rho = 2.7 \times 10^3\,\mathrm{kg/m^3}$, and Poisson's ratio $v = 0.34$. The resisting force of the damper is $F = 21.6\,\mathrm{N}$ when the damper has 3 pairs of magnets, and when the damper has two pairs of magnet, $F = 17.5\,\mathrm{N}$ as mentioned above.

4.2. Bending vibration

Figs. 4 and 5 show the comparison between the frequency response of displacements for the plate with or without the damper under a unit exciting force (1 N). Since the damper mass is attached to the plate, the natural frequency for the plate with the damper is sifted to the left in comparison with the result without damper (the damper is not attached to the plate, so the effects of damper mass is zero in the result without damper). Theoretically (from Fig. 4), the peak value of modal bending vibration without damper seems to be suppressed almost to zero by the presence of the damper with 3 pairs magnet. Experimentally (Fig. 5), amplitude reduction by the damper with 3 pairs magnet can be gained till 90% (from 11.8 to 1.2 mm).

4.3. Torsion and bending vibration

Figs. 6 and 7 depict the comparison between the theoretical and experimental results for torsion–bending vibrations. Since, there are some setting errors, and natural frequencies vary with

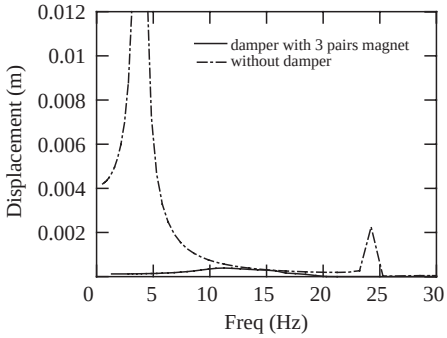

Fig. 4. Frequency response for bending vibrations (theoretical).

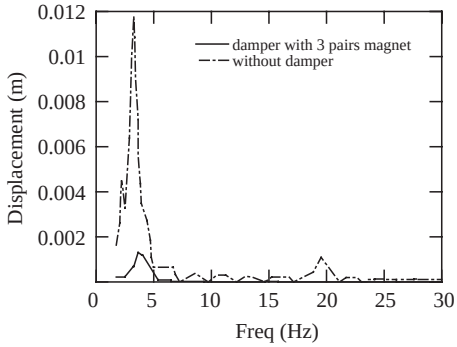

Fig. 5. Frequency response for bending vibrations (experimental).

fiction forces, experimental frequencies are somewhat smaller than the theoretical ones. Although there are a few differences, theoretical results are in good agreement with the theoretical from point of view of design engineering.

Figs. 6 and 7 shows clearly that the damper makes the most reducing effect with 3 pairs permanent magnet. From experimental result (Fig. 7), damper with 2 pairs magnet gives reduction of round 50% (from 73 to 37 mm) at first modal amplitude and round 64% (from 73 to 27 mm) by damper with 3 pairs magnet. Modal frequency of torsion vibration (Fig. 7, the second modal frequency) seem to be suppressed round 70% (from 18 to 5 mm) by the presence of the damper with 2 pairs magnet, and 90% (from 18 to 1.2 mm) by the damper with 3 pairs magnet.

The ordinary fluid damper needs a response time, because it needs the time of fluid flow in the orifice. While, since, the present damper is the friction damper, the friction force is constant under the magnetic field generated by the permanent magnets. This means that the response time of the damper is almost zero, so that the damper works in high frequency range. In addition, an ordinary piston-type fluid damper does not work for small displacement because of air compression in the damper. In our damper, the damper works in small displacement. These can be observed in the figures, because the second modal frequency is successfully suppressed in the experimental results.

In ordinary fluid dampers or rubber dampers do not work in low frequency range because the damping force is in proportion to velocity, while our damper also works in low frequency range

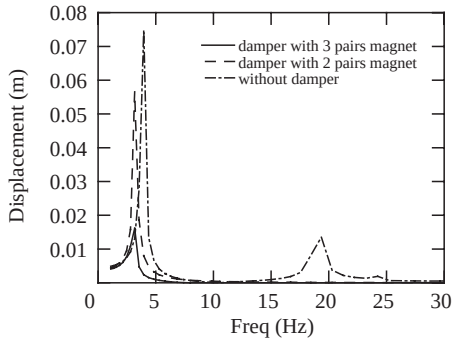

Fig. 6. Frequency response for bending–torsion vibrations (theoretical).

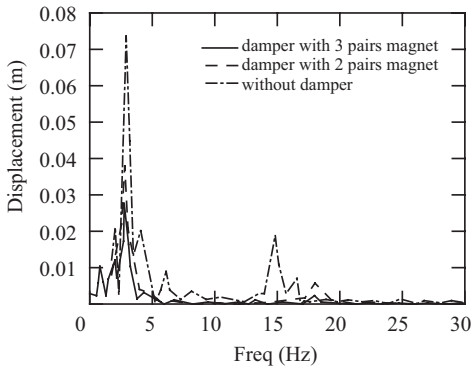

Fig. 7. Frequency response for bending–torsion vibrations (experimental).

because of the constant friction. This can be also observed in Figs. 4–7, because the vibration amplitude is attenuated in low frequency range.

In this theory, since the air damping is neglected, the theoretical amplitude is infinity when the plate has no damper. Hence, the theoretical amplitude at resonance does not coincide with the experimental one.

The resisting force of our damper is generated by permanent magnets, which do not consume electric energy, and the damper is maintenance free because of using passive type. Hence, our damper satisfies all requirements for the damper stated in Section 2.

5. Conclusion

This study discusses a development of shear-type MR fluid damper for controlling vibration of flexible plates such as aircraft wings. In order to predict effect of the damper, vibration suppressions of the cantilever plates are discussed theoretically and experimentally.

As mentioned above, the advantage of our damper is as follows: (1) the thickness is small, (2) the damping force can be designed, (3) since the damper is the friction type, and so it works for small displacement, (4) the damper is maintenance-free, and (5) the damper does not consume control energy, because electric field is generated by permanent magnets. By using the damper, plate vibrations are significantly attenuated. Hence, the damper satisfies all conditions for the plate vibration control damper such as aircraft damper, and its effect is enough.

The theoretical analyses for the damper and the vibration for the plate seem to be valid, so that the analytical results may be applied to the vibration design of plates.

Appendix A

The functions and coefficients are as follows:

$$\phi_m(X) = \cosh \xi_m X - \cos \xi_m X - a_m \sinh \xi_m X + a_m \sin \xi_m X,$$
$$\phi_m^{(1)}(X) = \xi_m(\sinh \xi_m X + \sin \xi_m X - a_m \cosh \xi_m X + a_m \cos \xi_m X),$$
$$\phi_m^{(2)}(X) = \xi_m^2(\cosh \xi_m X + \cos \xi_m X - a_m \sinh \xi_m X - a_m \sin \xi_m X),$$
$$\phi_m^{(4)}(X) = \xi_m^4 \phi_m(X),$$

where

$$X = x/a, \quad a_1 = 0.734096, \quad a_2 = 1.018466, \quad a_3 = 0.999225,$$
$$a_4 = 1.000034, \quad a_m = 1 \ (m \geqslant 5),$$
$$\xi_1 = 1.875104, \quad \xi_2 = 4.694091, \quad \xi_3 = 7.854757, \quad \xi_4 = 10.995541,$$
$$\xi_m = \frac{(2m-1)\pi}{2} \quad (m \geqslant 5),$$
$$Y = y/l, \quad \psi_0(Y) = 1, \quad \psi_0^{(1)}(Y) = 0, \quad \psi_0^{(2)}(Y) = 0, \quad \psi_0^{(3)}(Y) = 0,$$
$$\psi_0^{(4)}(Y) = 0 \quad (n = 0),$$

$$\psi_n(Y) = \mathrm{e}_n\left\{ Y^6 - 5Y^4 - 30\left(\frac{1}{n\pi}\right)^2(\cos n\pi Y - 1)\right\} + \mathrm{e}_n^*\left\{ Y^5 - \frac{10}{3}Y^3 + 40(-1)^n\left(\frac{1}{n\pi}\right)^3 \sin n\pi Y\right\},$$

$$\psi_n^{(1)}(Y) = \mathrm{e}_n\left\{6Y^5 - 20Y^3 - 30\left(\frac{1}{n\pi}\right)\sin n\pi Y\right\} + \mathrm{e}_n^*\left\{5Y^4 - 10Y^2 + 40(-1)^n\left(\frac{1}{n\pi}\right)^2 \cos n\pi Y\right\},$$

$$\psi_n^{(2)}(Y) = \mathrm{e}_n(30Y^4 - 60Y^2 + 30\cos n\pi y) + \mathrm{e}_n^*\left\{20Y^3 - 20Y - 40(-1)^n\left(\frac{1}{n\pi}\right)\sin n\pi Y\right\},$$

$$\psi_n^{(3)}(Y) = \mathrm{e}_n(120Y^3 - 120Y - 30n\pi \sin n\pi Y) + \mathrm{e}_n^*\{60Y^2 - 20 - 40(-1)^n\cos n\pi Y\},$$

$$\psi_n^{(4)}(Y) = \mathrm{e}_n\{360Y^2 - 120 - 30(n\pi)^2\cos n\pi Y\} + \mathrm{e}_n^*\{20Y + 40(-1)^n n\pi \sin n\pi Y\} \quad (n \geqslant 1)$$

and where

$$\mathrm{e}_n = \begin{cases} 1 & (n\text{: odd}), \\ 0 & (n\text{: even}), \end{cases} \quad \mathrm{e}_n^* = \begin{cases} 0 & (n\text{: odd}), \\ 1 & (n\text{: even}). \end{cases}$$

References

[1] J.C. Snowdon, A.A. Wolf, R.L. Kerlin, The cruciform dynamic vibration absorber, *The Journal of the Acoustical Society of America* 75 (1984) 1792–1799.

[2] H. Yamaguchi, H. Saito, Vibration of beams with an absorber consisting of a viscoelastic solids and beam, *Earthquake Engineering and Structural Dynamics* 12 (1984) 469–479.

[3] K. Nagaya, H. Kojima, On a magnetic damper consisting of a circular magnetic flux and a conductor of arbitrary shape (Part 1: Derivation of damping coefficients), *American Society of Mechanical Engineers Journal of Dynamic Systems, Measurement and Control* 106 (1984) 46–51.

[4] K. Nagaya, On a magnetic damper consisting of a circular magnetic flux and a conductor of arbitrary shape (Part 2: applications and numerical results), *American Society of Mechanical Engineers Journal of Dynamic Systems, Measurement and Control* 106 (1984) 52–55.

[5] D.H. Consalves, R.D. Neilson, A.D.S. Barr, The dynamics and design of a non-linear vibration absorber. Proceedings of the Institution of Mechanical Engineers, Part C, *Journal of Mechanical Engineering Science* 207 (1993) 363–374.

[6] J. Lee, Optimal weight absorber designs for vibrating structures exposed to random excitations, *Earthquake Engineering and Structural Dynamics* 19 (1990) 1209–1218.

[7] K. Nagaya, Y. Li, Method for reducing sound radiated from structures using vibration absorbers optimized with neural network, *Journal of Acoustical Society of America* 104 (1998) 1466–1473.

[8] K. Nagaya, L. Li, Control of sound noise radiated from a plate using dynamic absorbers under the optimization by neural network, *Journal of Sound and Vibration* 208 (1997) 289–293.
[9] G. Lee, J. Gina, G. Ahmad, G.H. Lucas, Integrated passive/active vibration absorber for multistory buildings, *Journal of Structural Engineering* 123 (1997) 499–504.
[10] N.P. Patten Wiliam, L. Sack Ronald, Q. He, Controlled semiactive hydraulic vibration absorber for bridges, *Journal of Structural Engineeering* 122 (1996) 187–192.
[11] K. Nagaya, A. Kurusu, S. Ikai, Y. Shitani, Vibration control of a structure by using a tunable absorber and optimal vibration absorber under auto-tuning control, *Journal of Sound and Vibration* 228 (4) (1999) 773–792.
[12] A. Baz, J. Ro, Vibration control of plates with active constrained layer damping, *Journal of Smart Materials and Structures* 5 (3) (1996) 272–280.
[13] A.M. Sadri, et al., active vibration control of isotropic plates using piezoelectric actuators, *Proceedings of the Sixth International Conference on Recent Advances in Structural Dynamics*, 1997, pp. 14–17.
[14] Y. Kim, D. Kum, C. Nam, Simultaneous structural/control optimum design of composite plate with piezoelectric actuators, *Journal of Guidance, Control, and Dynamics* 20 (6) (1997) 1111–1117.
[15] W. Shields, J. Ro, A. Baz, Control of sound radiation from a plate into an acoustic cavity using active piezoelectric-damping composites, *Journal of Smart Materials and Structures* 7 (1) (1998) 1–11.
[16] Y. Kim, I. Kim, C. Lee, C. Moon, Active suppression of plate vibration with piezoceramic actuator/sensor using multiple adaptive feedforward with feedback loop control algorithm, *SPIE Conference on Mathematics and Control in Smart Structures* 3667 (53) (1999) 553–564.
[17] S.A. Austin, The vibration damping effect of an electrorheological fluid, *American Society of Mechanical Engineers Journal of Vibration and Acoustics* 5 (1) (1993) 135–140.
[18] R.T. Bonnecaze, J.F. Brady, Yield stresses in electrorheological fluids, *Journal of Rheology* 36 (1) (1992) 73–113.
[19] J.M. Ginder, S.L. Cecccio, The effect of electrical transients on the shear stress in electrorheorlogical fluids, *Journal of Rheology* 39 (1) (1995) 211–234.
[20] Y. Choi, A.F. Sprecher, H. Conrad, Active vibration control of intelligent composite laminated structures incorporatig and electro-rheological fluid, *Journal of Intelligent Material Systems and Structure* 7 (4) (1996) 411–419.
[21] Y. Cho, A.F. Sprecher, H. Conrad, Response of electro-rheological fluid-filled laminate composites to forced-vibration, *Journal of Intelligent Material Systems and Structure* 3 (1) (1992) 17–29.
[22] S.-B. Choi, Vibration control of a flexible structure using ER damper, *American Society of Mechanical Engineers Journal of Dynamic Systems, Measurement and Control* 121 (1999) 134–138.
[23] K.W. Wang, Y.S. Kim, D.B. Shea, Structural vibration control via electrorheological-fluid-based actuators with adaptive viscous and frictional damping, *Journal of Sound and Vibration* 177 (2) (1994) 227–237.
[24] M.R. Jolly, Pneumatic motion control using megneto-rheogical fluid technology, *Proceedings of the 27th International Center for Actuators and Transducer Symposium on Smart Actuators*, State College, PA, 1999, pp. 22–23.
[25] S.J. Dyke, B.F. Spencer, et al., Seismic response reduction using MR Damper, *Proceeding of the IFAC World Congress*, San Francisco, CA, 1996, pp. 145–150.
[26] T. Nakagawa, A. Yamada, Design for a novel MRF semi-active damper and certification of the nonlinear controllers effects, *IEEE Transactions on Magnetics* 35 (5) (1999) 3604–3606.